Label-free proteomic analysis of the hydrophobic membrane protein complement in articular chondrocytes: a technique for identification of membrane biomarkers

Csaba Matta, Xiaofei Zhang, Susan Liddell, Julia R. Smith & Ali Mobasheri

Biomarkers

Taylor & Francis
Taylor & Francis Group

RESEARCH ARTICLE

Label-free proteomic analysis of the hydrophobic membrane protein complement in articular chondrocytes: a technique for identification of membrane biomarkers

Csaba Matta[1,2*#], Xiaofei Zhang[3*#†], Susan Liddell[3], Julia R. Smith[4], and Ali Mobasheri[1,5,6#]

[1]Department of Veterinary Preclinical Sciences, School of Veterinary Medicine, Faculty of Health and Medical Sciences, University of Surrey, Guildford, Surrey, UK, [2]Department of Anatomy, Histology and Embryology, Faculty of Medicine, University of Debrecen, Debrecen, Hungary, [3]Proteomics Laboratory, School of Biosciences, University of Nottingham, Sutton Bonington, UK, [4]Bruker UK Limited, Coventry, UK, [5]Arthritis Research UK Centre for Sport, Exercise and Osteoarthritis, Arthritis Research UK Pain Centre, Medical Research Council and Arthritis Research UK Centre for Musculoskeletal Ageing Research, University of Nottingham, Queen's Medical Centre, Nottingham, UK, and [6]Center of Excellence in Genomic Medicine Research (CEGMR), King Fahd Medical Research Centre (KFMRC), Faculty of Applied Medical Sciences, King AbdulAziz University, Jeddah, Kingdom of Saudi Arabia

Abstract

Context: There is insufficient knowledge about the chondrocyte membranome and its molecular composition.
Objective: To develop a Triton X-114 based separation technique using nanoLC-MS/MS combined with shotgun proteomics to identify chondrocyte membrane proteins.
Materials and methods: Articular chondrocytes from equine metacarpophalangeal joints were separated into hydrophobic and hydrophilic fractions; trypsin-digested proteins were analysed by nanoLC-MS/MS.
Results: A total of 315 proteins were identified. The phase extraction method yielded a high proportion of membrane proteins (56%) including CD276, S100-A6 and three VDAC isoforms.
Discussion: Defining the chondrocyte membranome is likely to reveal new biomarker targets for conventional and biological drug discovery.

Introduction

Proteins that are embedded in or associated with biological membranes play critically important roles in a wide range of vital cellular functions including transport, cell–cell communication and signalling processes. As the plasma membrane (PM) acts as the first barrier to the extracellular environment, PM proteins enable cells to sense and respond to external stimuli in a specific manner – they include receptors; cell recognition, cell–cell or cell–matrix adhesion sites; enzymes; as well as channels, pores and transporters for ions, small molecules and nutrients (Cordwell & Thingholm, 2010). Based on domain predictions by different methods, membrane proteins comprise approx. 15–30% of the human proteome (Almen et al., 2009; Kabbani, 2008), highlighting the fundamental importance of membrane-associated physiological processes. PM proteins are also the primary targets of many of the drugs that are currently in our pharmaceutical arsenal; indeed, the majority (over 70%) of currently marketed drugs act on PM proteins (Almen et al., 2009; Rabilloud, 2003). The qualitative and quantitative composition of the PM proteome is known to be significantly altered during cellular differentiation and disease. Membrane proteins have the potential to be selective and sensitive biomarkers for disease progression and prognosis. Furthermore, membrane proteins that exhibit altered expression in disease states could be suitable candidates for the development of sensitive receptor-targeted imaging agents for non-invasive monitoring of biological and inflammatory processes (Dissoki et al., 2015; Samkoe et al., 2014; Sega & Low, 2008). Therefore, there is a critical need for the development of tools and technologies for identification and characterisation of membrane proteins to complement physiological methods for elucidating their functions. This combined approach will promote the discovery

*These two authors contributed equally to the work.
#Csaba Matta, Xiaofei Zhang and Ali Mobasheri are responsible for statistical design/analysis. E-mail: c.matta@surrey.ac.uk (C. Matta); stxxz4@nottingham.ac.uk (X. Zhang); a.mobasheri@surrey.ac.uk (A. Mobasheri).
†Present address: Department of Joint Surgery, Tianjin Hospital, Tianjin, People's Republic of China.
Address for correspondence: Ali Mobasheri, Faculty of Health and Medical Sciences, Duke of Kent Building, University of Surrey, Guildford, Surrey, GU2 7XH, United Kingdom. E-mail: a.mobasheri@surrey.ac.uk

of new and better drugs, and the development of novel treatment strategies of diseases.

Integral membrane proteins have an amphiphilic structure; apart from hydrophilic domains located on the external cytosolic or organellar surfaces, they also contain hydrophobic (membrane-spanning) regions that directly interact with the lipid bilayer of the membranes in which they are embedded. High-resolution and high-throughput proteomic techniques have been widely applied to study the PM proteome of various cell types [for a review please see Cordwell & Thingholm (2010)]. However, there are serious (mainly technical) limitations that currently hinder advances in this field. In addition to their very low relative abundance, their amphiphilic nature and poor solubility makes membrane proteins challenging to purify, identify and characterise on a proteomic scale. The use of non-ionic detergents (e.g. the Triton X series in which the number of hydrophilic oxyethylene units attached to the hydrophobic octylphenyl residue determines the specific physicochemical properties) has enabled the solubilisation and characterisation of these proteins. Their use is based on the principle that water-soluble proteins, unlike amphiphilic membrane proteins, show little or no interaction with these compounds; consequently, only integral membrane proteins form mixed micelles with non-ionic detergents (Bordier, 1981). The cloud point, the temperature at which phase separation occurs between the detergent and the aqueous phase, is at approximately 20 °C for Triton X-114, which makes its application particularly convenient in studies aimed at analysing integral membrane proteins (Bordier, 1981; English et al., 2012; Mathias et al., 2011).

In addition to the application of non-ionic detergents, a number of other approaches have been developed over the past decades for the selective enrichment of membrane proteins including precipitation and gradient centrifugation, biotinylation and affinity enrichment or the application of glycoproteomics [reviewed in Cordwell & Thingholm (2010)]. The main technical challenge remaining in the analysis of integral membrane subproteomes, however, is the ability to obtain high purity membrane protein samples without the presence of high abundance contaminating proteins from the cytoplasm or other intracellular organelles. Comprehensive analyses of the membrane protein complement (also known as the membranome) of distinct cell types are relatively scarce; this can at least partially be attributed to the challenges and limitations described above. It is particularly true for chondrocytes, the single cell type in articular cartilage that serves as a specialised load-bearing tissue with unique tribological properties such as a low-friction gliding surface and peculiar rheology in synovial joints. The extracellular matrix (ECM) of hyaline cartilage, in which chondrocytes are embedded, primarily consists of a meshwork of type II collagen fibres and other minor collagens (types VI, IX and XI); large aggregating proteoglycans (e.g. aggrecan) and their constituent glycosaminoglycans (GAGs); as well as high quantities of osmotically bound water (approx. 70% of the net weight of ECM) and counteracting cations attracted by the net negative charge of GAGs (Archer & Francis-West, 2003). Because of its avascular nature and the inability of mature chondrocytes to divide *in situ*, once damaged, articular cartilage seldom regenerates on its own. Therefore, lesions

due to either osteoarthritis (OA) or traumatic injuries are associated with progressive degeneration of articular cartilage, pain and disability. OA is still an unresolved clinical problem, and developing novel therapies or drug targets poses a major challenge (Mobasheri, 2013).
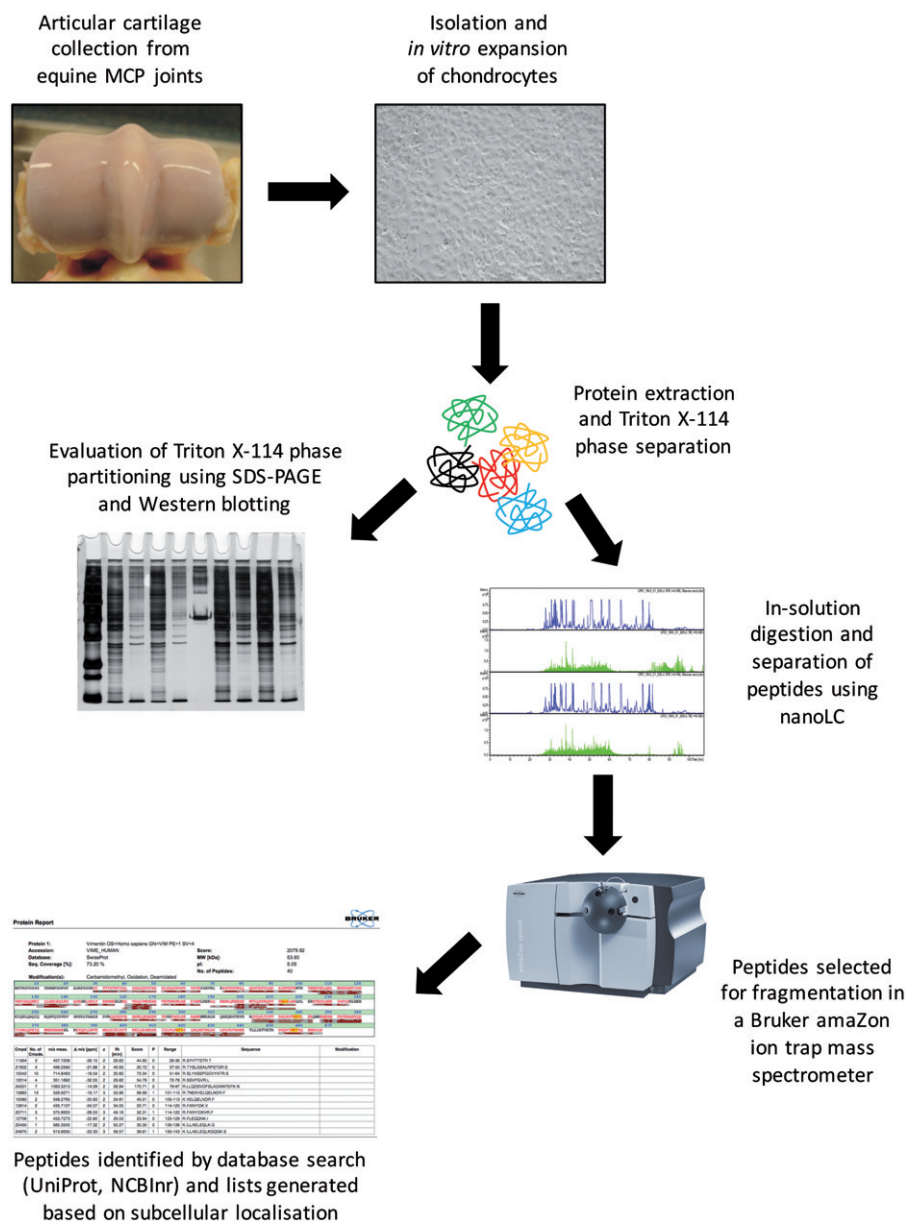
In order to identify proteins involved in pathological processes affecting the structure and function of articular cartilage such as OA, it is first necessary to characterise the normal protein complement of chondrocytes in healthy tissues. For proteomic studies, cartilage is very challenging as the chondrocyte, its sole cell type, forms only 1–2% of the volume of the tissue (Lambrecht et al., 2010). Although the proteome of healthy (Lambrecht et al., 2010; Ruiz-Romero et al., 2005) and OA-affected chondrocytes (Lambrecht et al., 2008; Ruiz-Romero et al., 2008; Tsolis et al., 2015), as well as the secretory profile (secretome) of a cartilage tissue explant model of OA (Williams et al., 2013) has been published, the ''hidden'' proteome, i.e. low-abundance membrane proteins or other poorly soluble proteins may have remained undiscovered in those studies. Here, we report a technique for profiling integral membrane proteins in primary equine articular chondrocytes using an optimised Triton X-114 phase partitioning technique and LC-MS/MS analysis for protein identification. To the best of our knowledge, this work represents the first and most comprehensive analysis of the integral membrane subproteome in chondrocytes reported. This technique allowed us to establish CD276, S100-A6 (calcyclin) and three VDAC isoforms as key components of the chondrocyte membranome.

Materials and methods

Isolation and culture of primary equine articular chondrocytes

Articular chondrocytes were isolated from equine articular cartilage. The animal used in this study was euthanized in a UK-based abattoir for research-unrelated purposes, and stunned before slaughter in accordance with Welfare of Animals (Slaughter or Killing) Regulations 1995. Ethical approval for the use of abattoir-derived animal tissues was obtained from the Ethics Committee of the School of Veterinary Science and Medicine, University of Nottingham, with input from members of the University of Nottingham Animal Welfare and Ethical Review Body (AWERB). After opening the metacarpophalangeal joint cavity under aseptic conditions and rinsing the articular cartilage surface with sterile physiological saline, articular cartilage shavings were taken from the distal end of the metacarpal bone using a sterile surgical blade and placed in serum-free DMEM (Thermo Fisher Scientific, Inc., Waltham, MA) supplemented with 4% Penicillin/Streptomycin solution (P/S, Sigma-Aldrich, St. Louis, MO) pre-warmed to 37 °C as described previously (Williams et al., 2013). The shavings (~100 µm thick, ~5 mm in diameter) were taken from the superficial part of macroscopically normal cartilage areas without any visible signs of degeneration, including discolouration, fibrillation and surface irregularities, to avoid the deep (calcified) layers of articular cartilage or the cartilage–bone interface. The surface of articular cartilage did not receive treatment prior to sampling to preserve the *lamina*

Figure 1. Schematic overview of the experimental design used in this study.

Articular cartilage collection from equine MCP joints

Isolation and *in vitro* expansion of chondrocytes

Protein extraction and Triton X-114 phase separation

Evaluation of Triton X-114 phase partitioning using SDS-PAGE and Western blotting

In-solution digestion and separation of peptides using nanoLC

Peptides selected for fragmentation in a Bruker amaZon ion trap mass spectrometer

Peptides identified by database search (UniProt, NCBInr) and lists generated based on subcellular localisation

splendens (the uppermost surface layer of articular cartilage) (Dunham et al., 1988).

Cartilage shavings were washed three times with sterile PBS containing 10% P/S. Articular chondrocytes were isolated by overnight incubation with 0.1% type II collagenase (from *Clostridium histolyticum*; Invitrogen, Carlsbad, CA) dissolved in serum-free DMEM containing 4% P/S solution at 37 °C. Following dissociation of cartilage shavings by trituration the solution was filtered through a 70-μm nylon mesh filter to yield a single cell suspension, and centrifuged at $800 \times g$ for 5 min at room temperature. After washing twice in serum-free DMEM, cells were resuspended in DMEM containing 10% foetal calf serum (FCS; Invitrogen) and 2% P/S solution, seeded into tissue culture flasks (Nunc; Thermo Fisher Scientific), and cultured in a CO_2 incubator at 37 °C. Cells were subcultured when they reached approx. 80% confluency. The media was changed on every second day. Cells from the second passage were used for further

experiments. A schematic overview of the experimental design is shown in Figure 1.

Sample preparation, phase partitioning using triton X-114, and methanol/chloroform extraction

Approximately 80% confluent cultures of primary equine articular chondrocytes from passage 2 were washed with PBS, then 2 mL of PBS containing 80 μL of protease inhibitor cocktail (25×, Sigma-Aldrich) was added to the flasks. The flasks were placed on ice, and cells were liberated using a cell scraper (Greiner, Stonehouse, UK). The solution was centrifuged (at $850 \times g$ for 2 min, room temperature), and the pellet was resuspended in 600 μL of PBS containing 24 μL of 25 × protease inhibitor cocktail. After incubating on ice for 15 min, the suspension was transferred into a glass homogeniser and the cells were lysed.

Following the addition of Triton X-114 (Sigma-Aldrich) at a final concentration of 0.75%, the lysate was incubated on ice

for 30 min with vortexing every 5 min. After centrifugation (30 min, 10 000 ×*g*, 4 °C) the supernatant was retained and incubated at 37 °C for 5 min, and then on ice for 15 min. The sample was centrifuged again (30 min, 10 000 ×*g*, 4 °C) and the supernatant was incubated at 37 °C for 5 min. Following centrifugation for 3 min (1000 ×*g*, room temperature), two layers appeared. The upper layer (aqueous phase) contained the hydrophilic proteins, the lower layer (detergent phase) contained the hydrophobic proteins. To maximise the recovery of membrane proteins, the upper layer was extracted further by adding Triton X-114 at a final concentration of 0.75% and the phase partitioning procedure was repeated. Finally, the two lower layers were combined together to constitute the hydrophobic fraction, and the upper layer was treated as the hydrophilic fraction.

To remove Triton X-114 from the samples, four times the sample volume of methanol (Thermo Fisher Scientific) was added to both fractions. After centrifugation at 15 000 ×*g* for 10 s at room temperature, two times the original sample volume of chloroform (Sigma-Aldrich) was added. The mixture was centrifuged again, and after adding three times the original sample volume of HPLC grade water, the sample was centrifuged for 5 min (15 000 ×*g*, room temperature). The proteins accumulated at the interface between the two layers formed during the last centrifugation step. Following removal of the upper layer, three times the sample volume of methanol was added, and after spinning for 5 min (15 000 ×*g*, 4 °C), the pellet containing the proteins was retained and air-dried.

Quantification of proteins

After methanol/chloroform extraction, the pellets were dissolved in sample resuspension buffer containing 4% SDS (Bio-Rad Laboratories, Inc., Hercules, CA), 0.2 M Tris pH 7.4 (Bio-Rad) and 0.15 M NaOH (Thermo Fisher Scientific). Protein concentration in the samples was determined using the Bio-Rad DC Protein Assay Kit according to the manufacturer's protocol (Bio-Rad). The absorbance of the assayed samples at 655 nm was read using a Bio-Rad Benchmark Microplate Reader.

Polyacrylamide gel electrophoresis (SDS–PAGE)

Loading buffer containing 4 × Laemmli buffer and 3 M dithiothreitol (DTT; Bio-Rad) was added to each sample (typically, 4.8 μL 4 × Laemmli buffer and 1.2 μL 3M DTT was added to 18 μL sample resuspension buffer), and then proteins were fractionated by SDS–PAGE on a 12% polyacrylamide gel. Proteins were initially run at 32 mA constant current, and once the dye front reached the bottom of the stacking gel, the current was increased to 45 mA. Protein bands were visualised by silver staining using a Hoefer Processor Plus automated gel stainer (Amersham, GE Healthcare Life Sciences, UK). The protocol for silver staining was performed as described previously (Yan et al., 2000).

Preparation and trypsin digestion of proteins for LC-MS/MS analysis: in-solution digestion

The protein pellets from the methanol/chloroform extraction step were resuspended in a solution of 50 mM ammonium

bicarbonate (AMBIC) (Sigma-Aldrich) and 10 mM DTT (Bio-Rad), and incubated at 37 °C for 30 min, vortexing every 10 min. Following the addition of iodoacetamide (IAA, Bio-Rad) at a final concentration of 55 mM, samples were incubated at 37 °C for 45 min in dark. Then, 1.2 mL of –20 °C acetone was added to each sample, and after mixing, the samples were incubated at 4 °C overnight. Protein precipitates were pelleted by centrifugation at 15 000 ×*g* for 5 min at 4 °C. Pellets were air-dried for 1 min, and then resuspended in 20 μL of trypsin buffer including 50 mM AMBIC and 10 ng/μL Trypsin Gold (Promega, Madison, WA). Samples were vortexed until the pellets were fully dissolved and then incubated at 37 °C for 16 h. Finally, 1 μL of formic acid (1%) was added to each sample to stop the reaction. Samples were stored at –80 °C until analysis.

LC-MS/MS analysis

Samples were injected into a 15 cm C18 Pepmap column using a Bruker (Coventry, UK) Easy-nanoLC UltiMate® (Bruker, Coventry, UK) 3000 RSLCnano chromatography platform with a flow rate of 300 nL/min to separate peptides. Three microlitres of each sample was injected into the HPLC column. After peptide binding and washing processes on the column, the complex peptide mixture was separated and eluted by a gradient of solution A (100% water + 0.1% formic acid) and solution B (100% ACN + 0.1% formic acid) over 115 min, followed by column washing and re-equilibration. The peptides were delivered to a Bruker (Coventry, UK) amaZon ETD ion trap instrument (Bruker, Coventry, UK). The top five most intense ions from each MS scan were selected for fragmentation. The nanoLC-MS/MS analysis was performed three times on the samples (all triplicates).

Peptide and protein identification, data analysis and bioinformatics

Processed data were compiled into *.MGF files and submitted to the Mascot search engine (version: 2.4.1) and compared to mammalian entries in the SwissProt and NCBInr databases. The data search parameters were as follows: two missed trypsin cleavage sites; peptide tolerance, ±0.3 Da; number of $C^{13} = 1$; peptide charge, 1+, 2+ and 3+ ions. Carbamidomethyl cysteine was specified as a fixed modification, and oxidised methionine and deamidated asparagine and glutamine residues were specified as variable modifications. Individual ions Mascot scores above 50 indicated identity or extensive homology. Only protein identifications with probability-based protein family Mascot MOWSE scores above the significant threshold of >50 ($p < 0.05$) were accepted. After mass spectrometric identification, 315 proteins were classified manually using the UniProt (http://www.uniprot.org/) database, considering homologous proteins and further literature information. For many proteins, assigning a definitive cellular compartment and/or function was a difficult task because of the limitations in accurate predictions and lack of experimental evidence. Also, many proteins may actually reside in multiple cellular compartments. To assign identified proteins to specific organelles, the references to subcellular localisations in the

UniProt database, as well as gene ontology (GO) annotations were used.

Validation of selected membrane proteins by western blotting

Hydrophobic and hydrophilic protein samples were loaded onto Mini-Protean 3 gels. Approximately 20 µg protein per lane was separated by 7.5% SDS–PAGE gel for immunological detection of selected proteins. Proteins were transferred to PVDF membranes (Immun-Blot™ PVDF Membrane, Bio-Rad). After blocking in 5% non-fat dry milk in PBST, membranes were incubated with the anti-Na$^+$, K$^+$-ATPase primary antibody (diluted 1:100) in blocking solution at 4 °C overnight, with gentle rotation. Membranes were then incubated with the secondary antibody (anti-mouse labelled polymer HRP, DakoCytomation, 1:1000 dilution) in blocking solution at room temperature for 1 h. Membranes were developed by enhanced chemiluminescence reaction (Amersham) according to the instructions of the manufacturer and using auto-radiographic films (Hyperfilm, Amersham). Films were scanned on a calibrated densitometer (Bio-Rad GS800) operated by Quantity One version 4.4.1 software (Bio-Rad). Optical density of bands was determined using ImageJ version 1.47 (ImageJ, Bethesda, MD; http://imagej.nih.gov/ij); data were normalised to the value detectable in the hydrophilic fraction.

Results

Triton X-114 phase separation efficiently enriches membrane proteins from primary chondrocyte cultures

To confirm whether the Triton X-114 phase separation method was able to efficiently extract and enrich lipid-soluble membrane proteins from primary articular chondrocytes cultured *in vitro*, equal amounts of proteins (25 µg) from the hydrophobic and the hydrophilic fractions were loaded onto polyacrylamide gels. Following SDS–PAGE and silver staining, protein bands with clearly different patterns appeared in the gels with several strong bands present in the hydrophobic fraction only (Figure 2A). To validate the effectiveness of the Triton X-114 extraction method, western blot experiments were performed on both fractions to probe for the presence and relative abundance of a membrane-bound Na$^+$, K$^+$-ATPase. As seen in Figure 2B, the band for this protein in the hydrophobic pool was more than 2.6-fold stronger than that in the hydrophilic pool, demonstrating that lipid-soluble proteins were extracted and enriched in the hydrophobic fraction.

To investigate the protein content of the two fractions, trypsin-digested protein fractions were analysed by nanoLC-MS/MS using Bruker Easy-nanoLC chromatography and a Bruker amaZon ion trap instrument with shotgun proteomics methodologies. A total of 315 unique proteins were reliably ($p < 0.05$) identified in this study; 208 proteins were detected in the hydrophobic fraction and 192 proteins in the hydrophilic fraction, with 73 (23%) proteins present in both fractions. According to the subcellular localisation data in the UniProt database entries and gene ontology (GO)

annotations, in the hydrophobic pool 115 proteins (55%) were membrane proteins and only the remaining 93 proteins (45%) were non-membrane proteins. In contrast, only 38 proteins (20%) were listed as membrane proteins in the hydrophilic fraction, and the other 154 proteins (80%) were non-membrane proteins (Figure 2C). Based on the distribution of membrane versus non-membrane proteins in the two fractions, using the Triton X-114 phase separation method, we successfully extracted and enriched membrane proteins in lysates of primary articular chondrocytes.

Further analysis of the hydrophobic pool reveals various types of membrane proteins

Proteins identified in the hydrophobic fraction were further analysed according to subcellular localisation based on gene ontology (GO) annotation data in the UniProt database entries (Figure 3). Of the 115 membrane proteins in this pool, PM localisation was indicated for 64 proteins (56%), and the other 51 proteins (44%) were localised in organellar membranes. The PM proteins were further subdivided according to their main functions (Table 1). Eighteen proteins (28%) were transporters or involved in membrane/vesicle traffic; 11 and 10 proteins (17 and 16%) were adhesion molecules and proteins with enzyme functions, respectively; 15 proteins (23%) were receptors, and the remaining 10 PM proteins (16%) could not be assigned to any of the previous groups or their function was unknown.

The membrane proteins with other organellar distributions were also subdivided according to their subcellular localisations (Table 2). The majority (23 proteins; 45%) were localised in the membrane of the Golgi complex or the endoplasmic reticulum; 13 proteins (25%) were localised to exosome/lysosome/endosome/other vesicular membranes; another big portion (11 proteins; 22%) were mitochondrial membrane proteins; two proteins (4%) were nuclear membrane proteins; and the remaining two proteins (4%) were ambiguous in terms of specific subcellular localisation.

The majority of the non-membrane proteins in the hydrophobic pool were cytoplasmic/cytoskeletal proteins (46 proteins; 50%) and secreted (extracellular) proteins (19 entries; 20%). Other subcellular localisations included the lysosome/endosome (4 proteins; 4%), the mitochondrion (1 protein; 1%), the Golgi complex or the endoplasmic reticulum lumen (8 proteins; 9%), the nucleus (10 proteins; 11%), and the remaining five proteins were either contaminants or their subcellular localisation was ambiguous (5%; Figure 4 and Table 3).

The hydrophilic pool contains proteins with different solubility and subcellular distribution

The Triton X-114 phase separation technique effectively extracted and enriched lipid-soluble membrane proteins in the hydrophobic phase, and left comparably few membrane proteins (only 20%) in the hydrophilic fraction (Figure 2C). As in the case of the hydrophobic fraction, the majority of the 38 lipid-soluble membrane proteins were localised in the PM (25 proteins; 66%), whilst the others were localised in various

Figure 2. Validation of the efficacy of the Triton X-114 phase separation method. (A) Distribution of protein bands in the hydrophobic (1) and hydrophilic (2) fractions following phase partitioning in total lysates from primary equine articular chondrocyte cultures. After SDS–PAGE, protein bands were visualised using silver staining (M, molecular weight marker). Representative gel image. (B) Western blot experiment performed on both hydrophobic and hydrophilic fractions to probe for the presence and relative abundance of the membrane-bound Na^+, K^+-ATPase. Numbers below bands represent integrated densities determined by ImageJ freeware. Representative image. (C). The relative distribution of identified proteins following analysis by nanoLC-MS/MS based on their solubility in both hydrophobic and hydrophilic fractions. Numbers outside pie charts represent the actual numbers of proteins identified in each subgroup.

organellar membranes (Golgi complex/endoplasmic reticulum membrane, 16%; mitochondrial membrane, 8%; nuclear membrane, 2%; Figure 5 and Table 4).

Taken together, we have identified 78 unique PM proteins in equine articular chondrocytes in this work. Among them, 32 proteins possessed receptor/adhesion functions; the most important ones are the cluster of differentiation (CD) proteins and integrins. Furthermore, 21 PM proteins with transporter functions were detected in articular chondrocytes (Tables 1 and 4).

The non-membrane protein complement in the hydrophilic fraction comprised 154 proteins, the majority of which (77 proteins; 50%) were cytoplasmic/cytoskeletal proteins. Also in good correlation with the non-membrane protein distribution observed in the hydrophobic samples, the secreted (extracellular) and the nuclear proteins were the second and third largest groups in this fraction (23 proteins, 15%; and 22 proteins, 14%, respectively). Other subcellular localisations included the lysosome/endosome (5 proteins; 3%), the mitochondrion (6 proteins; 4%), the Golgi complex or the endoplasmic reticulum lumen (13 proteins; 9%), and the

remaining eight proteins were either contaminants or their subcellular localisation was not determined (5%; Figure 5 and Table 5).

Discussion

The application of mass spectrometry (MS) has recently become an important tool in cartilage biology as it offers numerous advantages over more conventional biochemical approaches such as western blotting. To date, a number of proteomic studies have been performed on cartilage tissue and on chondrocytes, confirming that this analytical tool is particularly suitable for high-throughput and large-scale analysis of the protein complement in health and disease [reviewed in Hsueh et al. (2014) and Williams et al. (2011)]. The first proteomic study carried out on normal human knee articular chondrocyte cultures aimed at creating a two-dimensional gel electrophoresis (2-DE) reference map and generated 93 unique protein identities (Ruiz-Romero et al., 2005). A 1-D SDS–PAGE approach combined with MS/MS resulted in the identification of over 100 different proteins

Figure 3. Subcellular distribution of the identified membrane proteins in the hydrophobic fraction. PM proteins were further classified according to their main function based on GO annotations. Numbers outside pie charts represent the actual numbers of proteins identified in each subgroup.

Membrane protein distribution
(hydrophobic pool)

64 / 51

☐ Plasma membrane/surface proteins (56%)
☐ Proteins with subcellular organellar membrane localisation (44%)

Plasma membrane proteins:
functional distribution
(hydrophobic pool)

10, 18, 15, 11, 10

☐ Transporters, membrane/vesicle traffic (28%)
☐ Adhesion molecules (17%)
☐ Enzymes (16%)
☐ Receptors (23%)
☐ Other/miscellaneous (16%)

Organellar membrane protein
distribution
(hydrophobic pool)

2, 2, 13, 11, 23

☐ Exosome/lysosome/endosome/vesicle membrane (25%)
☐ Golgi/ER membrane (45%)
☐ Mitochondrial membrane (22%)
☐ Nuclear membrane (4%)
☐ Other/miscellaneous (4%)

from human knee cartilage supernatants (Garcia et al., 2006). In the first large-scale MS analysis of human articular cartilage, which was designed to extract both extracellular and intracellular proteins from samples depleted of highly abundant ECM proteins such as collagens and aggrecan to allow the detection of less abundant proteins, a total number of 814 distinct proteins were identified (Wu et al., 2007). In a more recent study, the proteome of articular chondrocytes from healthy and OA patients using high resolution label-free MS was analysed, leading to the identification of ~2400 proteins (Tsolis et al., 2015).

Despite these studies and the impressive number of proteins identified, our knowledge about the proteome of cartilage and its resident cell, the chondrocyte, can still be improved. One significant drawback is that at least in some of the studies the identified proteins have not been properly analysed in terms of subcellular locations and/or functions. In addition, the majority of proteins identified in these studies were located in the ECM because of their high abundance relative to cellular proteins in chondrocytes. More specifically, the ''hidden'' proteome, which comprises low abundance proteins and/or is not accessible by standard methods, is still poorly characterised. In a study that combined extensive prefractionation followed by electrospray ionisation mass spectrometry (ESI-MS/MS), 779 unique proteins expressed by cultured chondrocytes were identified, of which 203 were annotated to the membrane (Lambrecht et al., 2010). However, the authors did not carry out a detailed analysis with respect to specific subcellular location and/or function of the identified membrane proteins, making further data interpretation attempts challenging.

Therefore, the aim of this study was to extend the current knowledge of the chondrocyte proteome by using the Triton X-114 phase separation technique to discover the membrane

Table 1. Functional classification of PM proteins in the hydrophobic fraction identified in equine articular chondrocytes based on GO annotations.

#	Name	Accession No.*	Mascot score	Seq. coverage (%)	No. of matched peptides
	Transporters, membrane/vesicle traffic				
1	Voltage-dependent anion-selective channel protein 1	VDAC1	383	36.7	8
2	Voltage-dependent anion-selective channel protein 2	VDAC2	313	25.9	6
3	Voltage-dependent anion-selective channel protein 3	VDAC3	139	12.0	3
4	Ras-related protein Rab-5B	RAB5B	134	15.8	3
5	Ras-related protein Rab-5C	RAB5C	164	16.2	3
6	Ras-related protein Rab-8A	RAB8A	135	17.4	3
7	Ras-related protein Rab-8B	RAB8B	145	17.4	3
8	Ras-related protein Rab-9A	RAB9A	61	10.4	1
9	Membrane-associated progesterone receptor component 2	PGRC2	178	17.0	4
10	Annexin A1	ANXA1	125	9.2	2
11	Dolichyl-diphosphooligosaccharide–protein glycosyltransferase 48 kDa subunit	OST48	86	4.6	2
12	Solute carrier family 2, facilitated glucose transporter member 1	GTR1	118	6.3	3
13	Solute carrier family 2, facilitated glucose transporter member 3	GTR3	74	4.0	3
14	Caveolin-1	CAV1	69	11.8	1
15	Monocarboxylate transporter 1	MOT1	75	2.4	1
16	PREDICTED: Melanotransferrin (CD228 antigen)	MFI2	64	4.5	2
17	PREDICTED: Equilibrative nucleoside transporter 1 isoform X1	SCL29A1	67	5.5	2
18	PREDICTED: Synaptosomal-associated protein 23	SNAP23	57	11.4	1
	Adhesion molecules				
1	Integrin alpha-5 (CD49e antigen, Fibronectin receptor alpha subunit; fragment)	ITA5	97	6.5	2
2	Integrin alpha-V (CD51 antigen, Vitronectin receptor alpha subunit)	ITAV	84	3.2	3
3	Integrin beta-1 (CD29 antigen, Fibronectin receptor beta subunit)	ITB1	753	22.4	16
4	Thrombospondin-1	TSP1	435	9.7	9
5	RA175 (Cell adhesion molecule 1)	CADM1	58	5.5	1
6	CD151 antigen (Tetraspanin-24)	CD151	79	5.9	2
7	CD166 antigen (ALCAM, Fragment)	CD166	125	8.4	3
8	CD107 antigen (Lysosome-associated membrane glycoprotein)	LAMP2	53	2.0	2
9	PREDICTED: CD9 antigen (tetraspanin-29)	CD9	88	10.4	2
10	PREDICTED: integrin alpha-3 isoform 2 (CD49c antigen)	ITA3	60	1.2	1
11	PREDICTED: integrin beta-3 (CD61 antigen)	ITB3	57	0.8	1
	Receptors				
1	Protein S100-A6 (Calcyclin)	S10A6	277	53.3	4
2	CD44 antigen (Hyaluronan receptor)	CD44	260	15.3	5
3	CD63 antigen (Tetraspanin-30)	CD63	55	2.5	1
4	CD81 antigen (Tetraspanin-28)	CD81	54	8.5	1
5	Cofilin-1	COF1	234	39.8	5
6	Myristoylated alanine-rich C-kinase substrate	MARCS	172	9.0	3
7	Cell division control protein 42 homologue	CDC42	154	6.5	3
8	CD71 antigen (Transferrin receptor protein 1)	TFR1	64	1.7	1
9	PREDICTED: Thy-1 membrane glycoprotein (CD90 antigen)	THY1	152	21.1	3
10	Basigin (CD147 antigen) precursor	BSG	100	13.7	3
11	PREDICTED: disintegrin and metalloproteinase domain-containing protein 9 isoform 1	ADAM9	83	1.7	1
12	P48 (Cytokine receptor-like factor 3)	CRLF3	80	6.8	2
13	Membrane steroid binding protein	gi|7689365	191	29.2	4
14	Mannose receptor, C type 2	MRC2	69	0.9	1
15	Lactadherin	MFGM	66	2.7	1
	Enzymes				
1	Protein disulfide-isomerase	PDIA1	320	11.8	5
2	Alpha-enolase	ENOA	295	24.4	7
3	CD73 antigen (5'-nucleotidase)	5NTD	160	12.0	5
4	Ras-related protein Rap-1b	RAP1B	146	19.0	3
5	Prolyl endopeptidase FAP	SEPR	130	5.3	3
6	Transforming protein RhoA	RHOA	146	24.9	4
7	TRAF2 and NCK-interacting protein kinase	TNIK	61	0.6	1
8	Thioredoxin-related transmembrane protein 1	TMX1	67	4.3	1
9	Rho GTPase-activating protein 21	RHG21	56	0.4	1
10	PREDICTED: adipocyte plasma membrane-associated protein isoform X1	APMAP	62	3.0	1
	Miscellaneous				
1	Brain acid soluble protein 1	BASP1	223	21.1	4
2	Guanine nucleotide-binding protein G(I)/G(S)/G(O) subunit gamma-12	GBG12	98	56.9	3
3	Receptor expression-enhancing protein 5	REEP5	86	11.6	2
4	CD276 antigen	CD276	55	10.8	2
5	Annexin A5	ANXA5	54	3.8	1
6	Tuberin	TSC2	54	0.4	1
7	PREDICTED: Tetraspanin-6 isoform X1	TSPAN6	105	7.8	2
8	PREDICTED: Matrix-remodeling-associated protein 7	MXRA7	79	20.3	1
9	PREDICTED: Protein lifeguard 3	TMBIM1	77	4.5	1
10	PREDICTED: Proteolipid protein 2	PLP2	72	18.4	2

*UniProt IDs are shown where available. In other cases, NCBInr accession numbers are shown.

Table 2. Subcellular distribution of membrane proteins in the hydrophobic pool identified in equine articular chondrocytes based on GO annotations.

#	Name	Accession No.*	Mascot score	Seq. coverage (%)	No. of matched peptides
	Exosome/lysosome/endosome/vesicle membrane				
1	Ras-related protein Rab-7a	RAB7A	538	60.9	10
2	Vesicle-associated membrane protein 3	VAMP3	239	38.5	3
3	Ras-related protein Rab-10	RAB10	164	22.5	4
4	14-3-3 protein theta	1433T	201	22.0	5
5	Cation-dependent mannose-6-phosphate receptor	MPRD	150	13.3	3
6	Syntaxin-7	STX7	144	19.9	5
7	Ras-related protein Rab-11B	RB11B	176	14.2	3
8	Ras-related protein Rab-14	RAB14	128	15.3	3
9	Vesicle-associated membrane protein 5	VAMP5	54	11.2	1
10	Lysosome membrane protein 2	SCRB2	115	2.7	1
11	Charged multivesicular body protein 6	CHMP6	51	6.5	1
12	PRA1 family protein 2	PRAF2	89	16.3	2
13	PREDICTED: glucosylceramidase isoform X2	GLCM	88	4.9	2
	Golgi/ER membrane				
1	Ras-related protein Rab-1A	RAB1A	301	35.6	6
2	Ras-related protein Rab-1B	RAB1B	266	25.9	5
3	Ras-related protein Rab-2A	RAB2A	213	24.5	4
4	Transmembrane emp24 domain-containing protein 2 (Fragment)	TMED2	83	10.7	2
5	Transmembrane emp24 domain-containing protein 5	TMED5	57	5.3	1
6	Transmembrane emp24 domain-containing protein 9	TMED9	116	14.9	3
7	Transmembrane emp24 domain-containing protein 10	TMEDA	228	22.4	5
8	Membrane-associated progesterone receptor component 1	PGRC1	149	11.8	2
9	Membrane-associated progesterone receptor component 2	PGRC2	178	17.0	4
10	Transmembrane emp24 domain-containing protein 4	TMED4	120	12.3	2
11	78 kDa glucose-regulated protein	GRP78	155	5.5	3
12	Translocon-associated protein subunit delta	SSRD	110	17.3	2
13	Surfeit locus protein 4	SURF4	93	8.2	2
14	Vesicular integral-membrane protein VIP36	LMAN2	58	3.4	1
15	Calnexin	CALX	78	2.2	1
16	B-cell receptor-associated protein 31	BAP31	85	8.1	2
17	Eukaryotic translation initiation factor 5A-1	IF5A1	53	10.4	2
18	Vesicle-associated membrane protein-associated protein A	VAPA	83	4.8	1
19	Vesicle-trafficking protein SEC22b	SC22B	53	5.6	1
20	PREDICTED: PRA1 family protein 3	PRAF3	89	16.0	3
21	lanosterol 14-alpha demethylase	CP51A	72	2.4	1
22	PREDICTED: golgin subfamily B member 1	GOGA1	69	0.4	1
23	PREDICTED: NADH-cytochrome b5 reductase 3-like isoform 1	gi|338721361	62	4.7	1
	Mitochondrial membrane				
1	Cytochrome c oxidase subunit 5A, mitochondrial	COX5A	197	30.9	4
2	ATP synthase subunit beta, mitochondrial	ATPB	235	16.7	7
3	ATP synthase subunit alpha, mitochondrial	ATPA	144	6.3	3
4	ATP synthase subunit delta, mitochondrial	ATPD	90	8.3	1
5	Apoptosis regulator BAX	BAX	70	5.7	1
6	Cytochrome c oxidase subunit 4 isoform 1, mitochondrial (Fragment)	COX41	59	10.3	1
7	Carbamoyl-phosphate synthase [ammonia], mitochondrial	CPSM	65	1.2	1
8	prohibitin-2	PHB2	63	4.0	1
9	Cytochrome c oxidase subunit 5B, mitochondrial	COX5B	61	3.3	2
10	cytochrome oxidase subunit 2	COX2	74	3.1	1
11	PREDICTED: mitochondrial fission 1 protein-like	gi|558166747	58	10.5	1
	Nuclear membrane				
1	PREDICTED: nesprin-1	SYNE1	73	0.1	1
2	PREDICTED: transmembrane protein 109 isoform X1	TMEM109	60	4.9	1
	Miscellaneous				
1	Peptidyl-prolyl cis–trans isomerase A	PPIA	241	43.3	5
2	PREDICTED: cell cycle progression protein 1 isoform X1	CCPG1	65	1.6	2

*UniProt IDs are shown where available. In other cases, NCBInr accession numbers are shown.

subproteome (the membranome). We have chosen to use equine articular chondrocytes in this study, for the horse is widely involved in occupational/sports activities and considered as an excellent animal model for human joint diseases (Aigner et al., 2010) and yet, current knowledge is limited and relates to only the protein complement of equine chondrocytes. The unique features of our study are as follows. First, to the best of our knowledge, this is the first application of LC-MS/MS proteomics to study the membrane protein complement of cultured articular chondrocytes. Second, a large proportion (133 proteins; 42%) of the 315 proteins identified in this work consisted of membrane

Non-membrane protein distribution (hydrophobic pool)

- ☐ Secreted/extracellular/exosome (20%)
- ☐ Cytoplasm/cytoskeleton (50%)
- ☐ Lyosome/melanosome/endosome (4%)
- ☐ Mitochondrion (1%)
- ☐ Golgi/ER lumen (9%)
- ☐ Nucleus (11%)
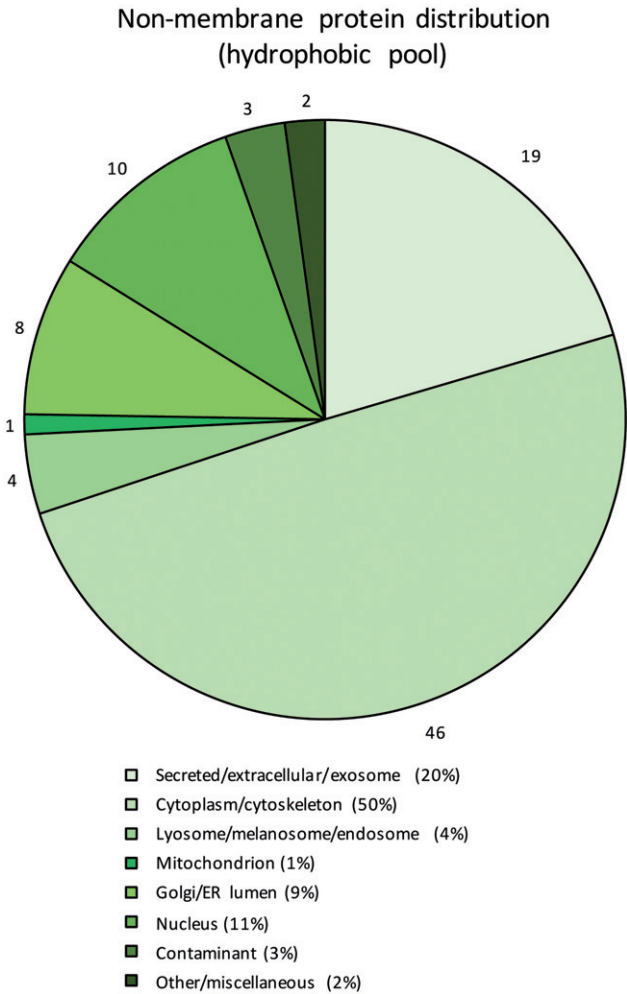- ☐ Contaminant (3%)
- ☐ Other/miscellaneous (2%)

Figure 4. Subcellular localisation of the identified non-membrane proteins in the hydrophobic fraction based on GO annotations. Numbers outside pie chart represent the actual numbers of proteins identified in each subgroup.

proteins, and for some of these only ambiguous data were available in chondrocytes [e.g. CD276, S100-A6 (calcyclin), VDACs]. The proportion of membrane proteins was even higher in the hydrophobic phase (55%). As far as the proportion of membrane proteins is concerned, our results are in a good agreement with those reported elsewhere (Hansson et al., 2010). The aim of that study was to characterise the human pancreatic islet membrane proteome by evaluating five different extraction procedures; while the proportion of membrane proteins in the total extracts was 35%, a considerably higher proportion (61%) of membrane proteins was identified following the use of membrane protein-enriching methods. It is also worth noting that the choice of method for extraction of membrane proteins had a strong influence on the number and identity of proteins detected in that analysis, and the hydrophobic phase of Triton X-114 phase separation was found to be the most efficient extraction method (Hansson et al., 2010). These results also underpin that appropriate sample preparation and pre-fractionation methods can increase the amount of identified proteins with specific properties in the MS/MS analysis of proteins in complex biological samples. It was for

that reason that we used the Triton X-114 phase separation method in this study.

Although a detailed description of the proteins identified in the chondrocyte membranome is beyond the scope of this article, a few important protein classes merit comment due to their potential involvement in chondrocyte homeostasis. We therefore restrict discussing our results to certain protein groups localised in the PM.

CD antigens and integrins

Cluster of differentiation (CD) proteins are four hydrophobic domain-containing cell surface membrane glycoproteins that mediate a range of cellular processes including development, differentiation, activation, growth and motility. Composed of alpha and beta subunits, integrins are integral PM receptors that mediate attachment between a cell and its surroundings. They transduce information from the ECM to the cell and integrin-mediated signalling pathways influence cell shape, mobility, differentiation and the cell cycle. The integrins identified in this study (integrin beta-1 [CD29], integrin alpha-5 [CD49e], integrin alpha-V [CD51], integrin alpha-3 [CD49c] and integrin beta-3 [CD61]) are in a complete agreement with what has been published earlier (Mobasheri et al., 2002a; Shakibaei et al., 2008; Woods et al., 1994). Our data also confirm reports on CD antigen expression in articular chondrocytes (Diaz-Romero et al., 2005). We found that equine articular chondrocytes express tetraspanins (CD9 [tetraspanin-19], CD63 [tetraspanin-30], CD81 [tetraspanin-28] and CD151 [tetraspanin-24]); CD44 (hyaluronan receptor); CD71 (transferrin receptor); CD90 (Thy-1); and CD166 (ALCAM). CD73, an ecto-5′-nucleotidase, which plays a crucial role in extracellular adenosine generation, has been reported to be involved in mechanotransduction pathways following cyclic compressive stimulation (Ode et al., 2013). CD107 (LAMP) expression has been recently reported in murine growth plate cartilage and cartilaginous nodules in embryonic limb bud-derived micromass cultures (Hatakeyama et al., 2014). CD147 (basigin; also known as extracellular matrix metalloproteinase inducer) is known to be extensively expressed by chondrocytes both in normal and OA cartilage (Orazizadeh & Salter, 2008). CD228 (melanotransferrin) has also long been known to facilitate the differentiation of prechondrogenic cells (Suardita et al., 2002). While CD276 has not been identified earlier in chondrocytes, it is known to be expressed in undifferentiated mesenchymal stem cells derived from Wharton's jelly (WJ-MSCs), even after osteogenic, adipogenic and chondrogenic differentiation (La Rocca et al., 2013).

S100 proteins

Of particular interest is protein S100-A6 (calcyclin) expression in equine articular chondrocytes. The S100 family of proteins consists of 24 members, which show cell-specific expression patterns and are involved in a wide range of cellular processes including proliferation, differentiation, apoptosis, Ca^{2+} homeostasis, energy metabolism, inflammation and migration/invasion through interactions with a variety of target proteins ranging from enzymes, cytoskeletal

Table 3. Subcellular distribution of non-membrane proteins in the hydrophobic pool identified in equine articular chondrocytes based on GO annotations.

#	Name	Accession No.*	Mascot score	Seq. coverage (%)	No. of matched peptides
	Secreted (extracellular)/exosome				
1	Alpha-2-macroglobulin	A2MG	914	15.8	19
2	Transgelin-2	TAGL2	426	47.7	9
3	Apolipoprotein D	APOD	188	24.3	6
4	Alpha-1-antiproteinase (Serpin A1, antitrypsin)	A1AT	220	9.4	5
5	Guanine nucleotide-binding protein G(I)/G(S)/G(T) subunit beta-1	GBB1	90	6.2	2
6	Annexin A2	ANXA2	83	7.7	2
7	Guanine nucleotide-binding protein subunit beta-4	GBB4	119	9.7	3
8	Galectin-1	LEG1	119	16.3	2
9	Pancreatic trypsin inhibitor	BPT1	52	13.0	1
10	Transthyretin	TTHY	95	19.0	2
11	SPARC	SPRC	190	25.3	5
12	Alpha-S1-casein	CASA1	72	10.3	2
13	Triosephosphate isomerase	TPIS	214	21.3	4
14	Hemopexin	HEMO	55	3.5	2
15	Apolipoprotein E	APOE	54	6.5	2
16	Hypothetical protein PANDA_010395 (lipocalin)	gi|281339160	152	5.9	1
17	PREDICTED: cell growth regulator with EF hand domain protein 1 isoformX1	gi|149727690	111	14.1	3
18	Complement component C4	CO4	63	11.6	1
19	PREDICTED: ovostatin-like	gi|344278152	57	1.1	1
	Cytoplasm/cytoskeleton				
1	Actin, cytoplasmic 1	ACTB	610	41.1	14
2	Tropomyosin alpha-4 chain	TPM4	538	32.7	10
3	Myosin light polypeptide 6	MYL6	337	52.3	8
4	60S acidic ribosomal protein P2	RLA2	334	60.0	5
5	Tropomyosin alpha-1 chain	TPM1	339	21.5	7
6	Tropomyosin beta chain	TPM2	319	18.0	6
7	Glyceraldehyde-3-phosphate dehydrogenase	G3P	271	15.9	4
8	Tropomyosin alpha-3 chain	TPM3	298	21.4	6
9	Tubulin alpha-1B chain	TBA1B	381	19.1	7
10	Transgelin	TAGL	136	16.4	3
11	L-lactate dehydrogenase A chain	LDHA	217	13.3	4
12	Pyruvate kinase PKM	KPYM	186	12.6	5
13	Tubulin alpha-1A chain	TBA1A	168	12.2	4
14	Heat shock protein beta-1 (hsp25, hsp27)	HSPB1	209	22.5	5
15	Peroxiredoxin-1	PRDX1	217	27.1	6
16	14-3-3 protein zeta/delta	1433Z	74	19.2	3
17	Tubulin beta-5 chain	TBB5	122	9.9	3
18	Profilin-1	PROF1	112	24.3	4
19	Fructose-bisphosphate aldolase A	ALDOA	178	13.7	3
20	Hsc70-interacting protein	F10A1	63	6.8	2
21	14-3-3 protein epsilon	1433E	57	11.4	2
22	Phosphoglycerate kinase 1	PGK1	83	6.7	2
23	Myosin-9	MYH9	100	0.6	1
24	Far upstream element-binding protein 2	FUBP2	103	4.6	3
25	Caldesmon	CALD1	82	3.9	2
26	14-3-3 protein beta/alpha	1433B	81	11.8	2
27	Guanine nucleotide-binding protein G(i) subunit alpha-2	GNAI2	77	7.9	2
28	60S acidic ribosomal protein P1	RLA1	64	14.0	1
29	40S ribosomal protein S12	RS12	63	19.7	2
30	Nuclease-sensitive element-binding protein 1	YBOX1	61	4.6	1
31	Calmodulin	CALM	59	22.1	2
32	Elongation factor 1-alpha 1	EF1A1	56	5.0	2
33	Heat shock cognate 71 kDa protein	HSP7C	134	6.3	3
34	Metallothionein-1A	MT1A	52	19.7	1
35	Protein S100-A1	S10A1	50	16.0	1
36	PREDICTED: protein S100-A11	gi|149751468	160	27.0	3
37	A-kinase anchor protein 9	AKAP9	82	0.3	1
38	PREDICTED: plasminogen activator inhibitor 1 RNA-binding protein isoform 1	gi|345800374	81	4.1	1
39	PREDICTED: peroxiredoxin-6	gi|149707887	80	17.9	3
40	hsp70A1	gi|193983	79	2.7	2
41	40S ribosomal protein S28	RPS28	79	30.4	2
42	PREDICTED: phosphatidylethanolamine-binding protein 1	gi|149720563	74	18.7	3
43	G-protein beta subunit	gi|51116	72	17.1	2
44	phosphoglycerate mutase	gi|189868	59	9.5	2
45	Stathmin	STMN1	59	15.1	2
46	Tropomyosin 3, gamma isoform 19-like protein	gi|528766928	268	18.6	7

Table 3. Continued

#	Name	Accession No.*	Mascot score	Seq. coverage (%)	No. of matched peptides
	Lysosome/melanosome/endosome				
1	Cathepsin D	CATD	218	15.6	7
2	Prosaposin	SAP	184	6.5	4
3	Cathepsin K	CATK	56	5.2	2
4	CLN2 protein (tripeptidyl peptidase 1)	TPP1	64	1.8	1
	Mitochondrion				
1	PREDICTED: Diablo homologue, mitochondrial-like	gi|345323079	69	4.1	1
	Golgi/ER lumen				
1	Reticulocalbin-3	RCN3	252	12.2	3
2	Glucosidase 2 subunit beta	GLU2B	129	4.3	2
3	Endoplasmin (hsp90beta1)	ENPL	123	2.5	2
4	Glucosidase 2 subunit beta	GLU2B	100	5.8	2
5	Calumenin	CALU	73	10.2	2
6	Serpin H1	SERPH	73	3.6	1
7	Calreticulin	CALR	65	3.1	1
8	Endoplasmic reticulum resident protein 29	ERP29	51	8.4	2
	Nucleus				
1	Far upstream element-binding protein 1	FUBP1	237	14.4	7
2	Prothymosin alpha	PTMA	198	21.8	4
3	Neuroblast differentiation-associated protein AHNAK	AHNK	166	0.8	4
4	Thioredoxin	THIO	130	2.1	2
5	Coiled-coil domain-containing protein 57	CCD57	67	0.8	1
6	Small ubiquitin-related modifier 2	SUMO2	54	12.6	1
7	PREDICTED: zinc finger protein 764-like	gi|558191623	66	2.7	1
8	PREDICTED: Fanconi anaemia group C protein	gi|348565316	56	1.6	1
9	PREDICTED: poly [ADP-ribose] polymerase 6 isoformX1	gi|545216657	206	4.9	2
10	Bromodomain adjacent to zinc finger domain protein 2A	BAZ2A	198	2.7	5
	Contaminants				
1	Keratin, type II cytoskeletal 1	K2C1	592	21.4	12
2	Serum albumin	ALBU	195	7.7	4
3	Trypsin	TRYP	75	7.8	2
	Miscellaneous				
1	PREDICTED: leptin receptor gene-related protein-like isoform X1	gi|545218045	79	11.5	1
2	Chain C, Ternary Complex Of A Calcineurin A Fragment, Calcineurin B, Fkbp12 And The Immunosuppressant Drug Fk506 (tacrolimus)	gi|1942335	65	12.1	1

*UniProt IDs are shown where available. In other cases, NCBInr accession numbers are shown.

subunits, receptors, transcription factors and nucleic acids [reviewed in Donato et al. (2013)]. In particular, S100-A6 may function as a Ca^{2+} sensor and modulator, contributing to Ca^{2+} signalling pathways. It is also implicated in cell proliferation and cytoskeletal dynamics, and known to have a potential role in cell responses to different stressors. Calcyclin was reported to be significantly upregulated in serially passaged adipose tissue-derived MSCs (Capra et al., 2012), which may correspond to previous data suggesting that it is frequently upregulated during proliferation and differentiation and it is induced by different growth factors. There are only sporadic data available relating to S100-A6 expression in chondrocytes. Its mRNA transcript has been shown to be downregulated following chondrogenic induction by BMP4 in ATDC5 cells, and it has also been identified in one of the chondrocyte proteome studies discussed earlier (Lambrecht et al., 2010).
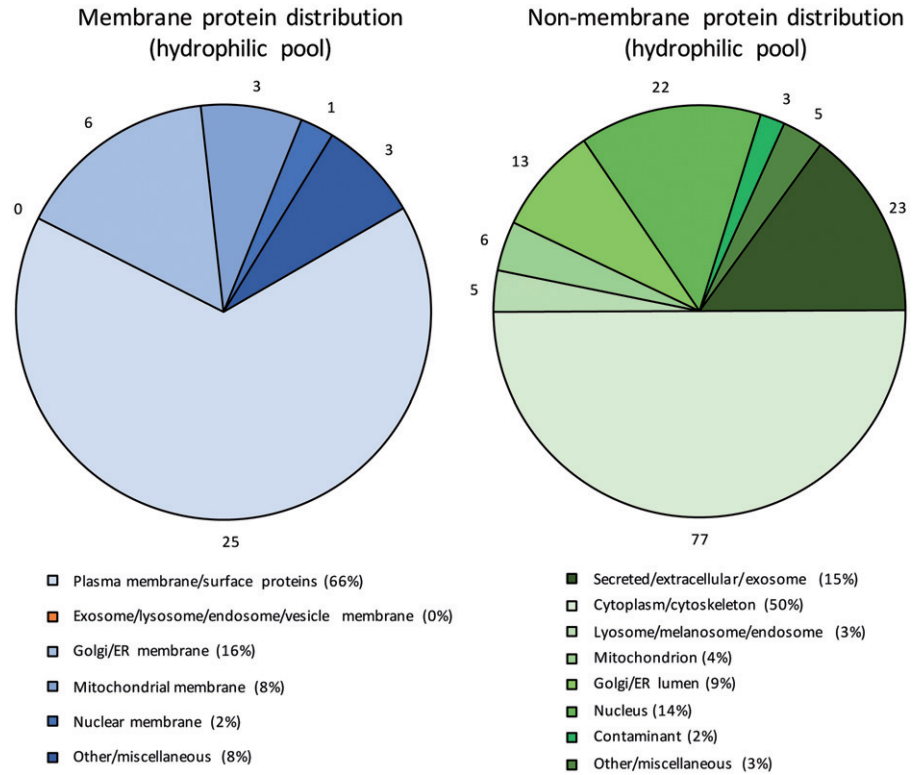
Other S100 proteins identified in this study include S100-A1 and S100-A11 (Tables 3 and 5). S100-A1 is localised in the cytoplasm where it is associated with cytoskeletal components and mitochondria. It can influence Ca^{2+} handling in cultured ventricular cardiomyocytes through interaction with the sarcoplasmic reticulum Ca^{2+}-ATPase and RyR2; it also modulates $Ca_V 1$ channel currents in a PKA-dependent manner. S100-A1 also regulates energy metabolism by stimulating fructose-1,6-biphosphate aldolase and inhibiting phosphoglucomutase and glycogen phosphorylase (Donato et al., 2013). Also localised in the cytoplasm, S100-A11 is reported to modulate cell growth *via* binding either to nucleolin or Rad54B (Donato et al., 2013). In particular, S100-A11 can activate the p38 MAPK pathway to accelerate chondrocyte hypertrophy and ECM catabolism that may promote OA progression (Cecil & Terkeltaub, 2008). Both S100-A1 and S100-A11 have been reported to be expressed and functional in chondrocytes (Donato et al., 2013; Patti et al., 1999), and both proteins were identified in a previous MS study (Lambrecht et al., 2010).

Transporters

Ion channels and transporters are essential components of chondrocytes that control the movement of ions and other small molecules across the PM. An increasing number of studies have reported the presence of an ever-expanding list of

Figure 5. Subcellular localisation of the identified membrane and non-membrane proteins in the hydrophilic fraction based on GO annotations. Numbers outside pie charts represent the actual numbers of proteins identified in each subgroup.

Membrane protein distribution (hydrophilic pool)

- ☐ Plasma membrane/surface proteins (66%)
- ☐ Exosome/lysosome/endosome/vesicle membrane (0%)
- ☐ Golgi/ER membrane (16%)
- ☐ Mitochondrial membrane (8%)
- ☐ Nuclear membrane (2%)
- ■ Other/miscellaneous (8%)

Non-membrane protein distribution (hydrophilic pool)

- ■ Secreted/extracellular/exosome (15%)
- ☐ Cytoplasm/cytoskeleton (50%)
- ☐ Lyosome/melanosome/endosome (3%)
- ☐ Mitochondrion (4%)
- ☐ Golgi/ER lumen (9%)
- ☐ Nucleus (14%)
- ■ Contaminant (2%)
- ■ Other/miscellaneous (3%)

ion channels and transporters in chondrocytes [reviewed in Barrett-Jolley et al. (2010) and Matta et al. (2015)]. Based on GO annotations, 21 proteins with transporter functions were identified in the PM in this study (Tables 1 and 4). Originally described as being localised in the outer mitochondrial membrane (Benz, 1994), voltage-dependent anion-selective channels (VDACs), also known as mitochondrial porins, form the pores that allow the transport of small hydrophilic solutes across the membrane. However, accumulating evidence support that VDACs can also be expressed in the PM (De Pinto et al., 2010), where they exhibit voltage-gated anion channel activity, and its electrophysiological phenotype is that of a maxi-chloride channel (Lewis et al., 2013). Although VDACs have not been unequivocally reported to be expressed and function in chondrocytes, the anion channel identified in some previous studies was the maxi-chloride channel, which is remarkably similar to the maxi-Cl⁻/VDAC channel (Sugimoto et al., 1996; Tsuga et al., 2002). Although all three VDAC proteins were identified in chondrocytes in our experiments and also by others (Lambrecht et al., 2010), further studies will need to functionally investigate the physiological and pathophysiological roles of these transporters in the chondrocyte PM.

The chloride intracellular channel (CLIC) proteins possess pH-dependent chloride ion channel activity. CLIC1 and CLIC4, in addition to other members of the CLIC family, are often referred to as "p64-related" proteins, and while they may localise to intracellular compartments (e.g. the nucleus), they also appear to be in the PM and could serve a role in secretion (Lewis et al., 2013). Once again, although the CLIC1 protein was identified in chondrocytes in this study and by others (Lambrecht et al., 2010), its presence

and function has not been unambiguously demonstrated earlier.

In addition to anion channels, glucose transporter (GLUT) proteins (facilitative glucose transporter 1 and 3; GLUT 1 and GLUT3) were also identified in our study. Glucose is a key metabolite and a structural precursor for articular cartilage and its transport has significant consequences for cartilage development and functional integrity. Our results are in a good agreement with previously published data (Mobasheri et al., 2002b), confirming here by proteomic techniques the expression of these two GLUT isoforms in articular chondrocytes.

Conclusion

In summary, studying the membranome profile of equine articular chondrocytes by LC-MS/MS following enrichment using Triton X-114 pre-fractionation has turned out to be an excellent approach to gain insight into proteins involved in a wide range of membrane-bound processes such as signal transduction, adhesion and transport of ions and other molecules. In spite of the significant enrichment of lipid-soluble membrane proteins in the hydrophobic phase, the proteins that are present in an extremely low abundance in chondrocytes such as the majority of ion channels and other transporter molecules in the PM remained undetectable. Although detergent-based phase partitioning enriches PM proteins relative to total soluble proteins, the membrane proteins in the ER, mitochondria and other organelles are also enriched; and the abundance of proteins in the contaminating organelles can interfere with the ability to detect PM proteins (Zhang & Peck, 2011). To mitigate these limitations, a

Table 4. Functional classification of PM proteins and other membrane proteins in the hydrophilic pool identified in equine articular chondrocytes based on GO annotations.

#	Name	Accession No.*	Mascot score	Seq. coverage (%)	No. of matched peptides	Function of PM protein
	Plasma membrane/surface proteins					
1	Thrombospondin-1	TSP1	811	14.3	14	Adhesion
2	Protein disulfide-isomerase	PDIA1	614	28.1	13	Enzyme
3	Alpha-enolase	ENOA	557	32.5	11	Enzyme
4	Annexin A1	ANXA1	468	39.9	10	Transporter
5	Cofilin-1	COF1	306	38.6	5	Receptor
6	Moesin	MOES	303	15.1	8	Adhesion
7	Annexin A5	ANXA5	258	19.1	6	Other (receptor)
8	Integrin beta-1 (CD29 antigen, Fibronectin receptor beta subunit)	ITB1	160	6.3	4	Adhesion
9	Protein disulfide-isomerase A6	PDIA6	147	14.1	4	Enzyme
10	Protein disulfide-isomerase A4	PDIA4	109	1.9	1	Enzyme
11	Prolow-density lipoprotein receptor-related protein 1	LRP1	76	0.5	2	Receptor
12	Annexin A4	ANXA4	58	5.6	2	Other (receptor)
13	40S ribosomal protein SA (Laminin receptor)	RSSA	57	4.4	1	Receptor
14	Procollagen-lysine,2-oxoglutarate 5-dioxygenase 2	PLOD2	53	1.9	1	Enzyme
15	Myristoylated alanine-rich C-kinase substrate	MARCS	52	4.5	1	Other
16	Cytoskeleton-associated protein 4	CKAP4	99	5.0	3	Receptor
17	Guanine nucleotide-binding protein subunit beta-2-like 1	GBLP	66	7.3	2	Other
18	Brain acid soluble protein 1	BASP1	52	5.7	1	Other
19	Talin-1	TLN1	418	3.1	8	Other (receptor)
20	PREDICTED: annexin A8 isoform X1	gi|149690688	127	12.8	3	Other
21	PREDICTED: alpha-2-macroglobulin receptor-associated protein	gi|545213509	116	7.3	2	Other
22	PREDICTED: chloride intracellular channel protein 1	gi|149732344	68	12.4	2	Transporter
23	PREDICTED: ADP/ATP translocase 2-like	gi|558210559	64	2.7	1	Transporter
24	PREDICTED: utrophin	gi|507925858	57	0.4	1	Other
25	Vacuolar protein sorting-associated protein 35	VPS35	65	1.6	1	Transporter
	Exosome/lysosome/endosome/vesicle membrane					
	Golgi/ER membrane					
1	78 kDa glucose-regulated protein	GRP78	734	30.0	15	
2	Peptidyl-prolyl cis-trans isomerase A	PPIA	268	43.3	7	
3	Peptidyl-prolyl cis-trans isomerase B	PPIB	174	21.3	4	
4	14-3-3 protein theta	1433T	122	13.9	3	
5	Calnexin	CALX	49	2.2	1	
6	PREDICTED: golgin subfamily B member 1 isoform 1	gi|466052157	62	0.3	1	
	Mitochondrial membrane					
1	ATP synthase subunit beta, mitochondrial	ATPB	120	4.5	2	
2	ATP synthase subunit alpha, mitochondrial	ATPA	89	6.1	2	
3	ATP synthase subunit delta, mitochondrial	ATPD	74	8.3	1	
	Nuclear membrane					
1	Nesprin-1	SYNE1	57	0.1	1	
	Miscellaneous					
1	DNA primase small subunit	gi|431914029	203	2.8	3	
2	PREDICTED: calpastatin isoform X5	gi|545185308	69	3.4	2	
3	CD209 antigen-like protein C	C209C	54	3.4	1	

*UniProt IDs are shown where available. In other cases, NCBInr accession numbers are shown.

combination of the Triton X-114 phase separation method with other membrane protein enrichment techniques could also be considered.

Our study confirms some previous findings and adds further proteins to the proteomic profile of equine articular chondrocytes. Some of the identified proteins including the CD276 antigen, S100-A6 (calcyclin) or VDACs have not been unambiguously reported before to be components of articular chondrocytes. However, there are certain limitations to this work. First and foremost, protein identifications were somewhat aggravated by the fact that our search results listed the same proteins several times but for different species (primarily human or bovine but no horse entries), suggesting that the protein was present in the sample and that the identification was made by virtue of the horse protein sharing homology with several other species. This is one of the disadvantages

when ''cross species matching'' is used to identify proteins. Another possible disadvantage of using equine articular chondrocytes is that there may be subtle differences between the two species and that the entirety of our results may not be directly applicable to human articular chondrocytes.

A more detailed and comprehensive insight into the chondrocyte membranome is likely to make a significant contribution to the development of novel drugs for arthritic diseases. The development and refinement of proteomics-based techniques will enable a better understanding of regulatory proteins and enhance the search for new drug targets. It may also help to discover novel cartilage disease-specific biomarkers. Thus, our data represent a significant addition to the comprehensive cartilage proteome database that is essential for understanding the molecular mechanisms underlying cartilage function and OA.

Table 5. Functional classification of non-membrane proteins in the hydrophilic pool identified in equine articular chondrocytes based on GO annotations.

#	Name	Accession No.*	Mascot score	Seq. coverage (%)	No. of matched peptides
	Secreted (extracellular), exosome				
1	Alpha-2-macroglobulin	A2MG	2098	37.0	45
2	Transgelin-2	TAGL2	475	44.2	7
3	Annexin A2	ANXA2	397	27.7	8
4	Triosephosphate isomerase	TPIS	337	30.5	6
5	Hemopexin	HEMO	270	17.9	7
6	Serotransferrin	TRFE	268	13.1	7
7	Alpha-1-antiproteinase	A1AT	254	10.3	5
8	Collagen alpha-1(I) chain	CO1A1	141	1.8	2
9	Myosin regulatory light chain RLC-A	MRLCA	127	22.7	3
10	Galectin-1	LEG1	109	22.2	3
11	Transthyretin	TTHY	91	19.0	2
12	Macrophage migration inhibitory factor	MIF	86	17.4	2
13	Complement C4 (Fragments)	CO4	63	3.6	2
14	Alpha-1-inhibitor 3	A1I3	59	0.8	1
15	Pancreatic trypsin inhibitor	BPT1	51	13.0	1
16	Connective tissue growth factor	CTGF	98	2.9	1
17	SH3 domain-binding glutamic acid-rich-like protein	SH3L1	62	7.9	1
18	Collagen alpha-5(VI) chain	CO6A5	58	0.2	1
19	Thrombospondin-2	TSP2	50	1.0	1
20	PREDICTED: heat shock protein HSP 90-alpha-like, partial	gi|507695623	99	3.8	2
21	PREDICTED: glia-derived nexin (Serpin E2)	gi|344268474	60	3.0	1
22	AM2 receptor	gi|49942	60	0.4	2
23	Semaphorin-3G precursor	gi|9910362	57	1.3	1
	Cytoplasm/cytoskeleton				
1	Tropomyosin alpha-4 chain	TPM4	902	47.6	15
2	Tropomyosin beta chain	TPM2	722	31.7	12
3	Tropomyosin alpha-3 chain	TPM3	639	34.7	10
4	Actin, cytoplasmic 1	ACTB	616	43.5	13
5	Tropomyosin alpha-1 chain	TPM1	584	32.4	11
6	Phosphoglycerate kinase 1	PGK1	555	42.7	13
7	L-lactate dehydrogenase A chain	LDHA	492	22.6	6
8	Heat shock cognate 71 kDa protein	HSP7C	486	17.7	10
9	Pyruvate kinase PKM	KPYM	463	23.7	10
10	14-3-3 protein epsilon	1433E	433	37.6	9
11	Fructose-bisphosphate aldolase A	ALDOA	423	27.7	9
12	Filamin-A OS = Homo sapiens	FLNA	406	4.3	8
13	Tubulin alpha-1B chain	TBA1B	358	20.2	7
14	Transgelin	TAGL	357	41.3	8
15	Myosin-9	MYH9	351	7.2	9
16	Glyceraldehyde-3-phosphate dehydrogenase	G3P	335	22.8	6
17	14-3-3 protein zeta/delta	1433Z	319	24.1	5
18	Tubulin beta-5 chain	TBB5	310	20.7	7
19	Phosphoglycerate mutase 1	PGAM1	271	27.2	5
20	Myosin light polypeptide 6	MYL6	249	52.3	7
21	Protein SET	SET	225	18.3	4
22	Elongation factor 1-alpha 1	EF1A1	222	11.3	6
23	Nuclease-sensitive element-binding protein 1	YBOX1	211	14.8	3
24	Glutathione S-transferase P	GSTP1	202	20.0	3
25	Phosphatidylethanolamine-binding protein 1	PEBP1	196	26.2	3
26	Peroxiredoxin-1	PRDX1	195	28.1	5
27	Profilin-1	PROF1	195	40.7	6
28	Alpha-actinin-4	ACTN4	193	6.0	5
29	L-lactate dehydrogenase B chain	LDHB	188	9.9	3
30	Caldesmon	CALD1	182	5.7	5
31	14-3-3 protein beta/alpha	1433B	174	18.3	4
32	Stathmin	STMN1	159	37.6	5
33	LIM and SH3 domain protein 1	LASP1	153	13.7	3
34	Elongation factor 2	EF2	147	4.7	4
35	L-lactate dehydrogenase C chain	LDHC	144	7.2	3
36	Heat shock 70 kDa protein 1A	HS71A	138	5.3	3
37	Heat shock protein HSP 90-beta	HS90B	128	4.7	3
38	14-3-3 protein gamma	1433G	112	6.1	2
39	Ferritin light chain	FRIL	109	16.0	2
40	Vinculin	VINC	107	2.5	2
41	Heat shock protein HSP 90-alpha	HS90A	100	4.9	3

Table 5. Continued

#	Name	Accession No.*	Mascot score	Seq. coverage (%)	No. of matched peptides
42	Calmodulin	CALM	97	33.6	4
43	Centromere protein F	CENPF	96	0.2	1
44	Nascent polypeptide-associated complex subunit alpha, muscle-specific form	NACAM	95	0.7	1
45	Ubiquitin	UBIQ	92	32.9	2
46	Peroxiredoxin-4	PRDX4	91	11.8	3
47	Peroxiredoxin-6	PRDX6	89	10.3	2
48	Titin	TITIN	81	0.0	2
49	Plastin-3	PLST	77	4.9	2
50	Nucleoside diphosphate kinase B	NDKB	69	17.1	2
51	40S ribosomal protein S28	RS28	69	17.4	1
52	Eukaryotic translation initiation factor 4B	IF4B	63	2.8	1
53	Hepatoma-derived growth factor	HDGF	61	4.2	1
54	Rho GDP-dissociation inhibitor 1	GDIR1	60	15.2	2
55	Fuctinin-3 (Fragment)	FUC3	59	84.6	2
56	Peptidyl-prolyl cis-trans isomerase FKBP1A	FKB1A	59	12.0	1
57	Eukaryotic translation initiation factor 4H	IF4H	55	5.2	1
58	Metallothionein-1A	MT1A	55	19.7	1
59	Heterogeneous nuclear ribonucleoprotein Q	HNRPQ	53	5.6	2
60	Rab GDP dissociation inhibitor alpha	GDIA	53	8.5	2
61	60S ribosomal protein L22	RL22	52	8.6	1
62	40S ribosomal protein S21	RS21	103	12.0	1
63	Myosin-10	MYH10	95	2.3	3
64	40S ribosomal protein S19	RS19	81	6.9	1
65	Ran-specific GTPase-activating protein	RANG	65	5.3	1
66	Peroxiredoxin-2	PRDX2	57	8.1	2
67	Plastin-2	PLSL	56	1.4	1
68	Prostaglandin E synthase 3	TEBP	50	8.1	1
69	Transitional endoplasmic reticulum ATPase	TERA	50	1.6	1
70	Tropomyosin 3, gamma isoform 19-like protein	gi|528766928	639	27.2	12
71	Striated-muscle alpha tropomyosin	gi|207349	590	34.2	12
72	PREDICTED: protein S100-A11	gi|149751468	148	27.0	3
73	PREDICTED: hsc70-interacting protein isoform X1	gi|149743058	113	7.3	2
74	PREDICTED: ubiquitin-60S ribosomal protein L40 isoform X1	gi|532055807	82	19.5	2
75	PREDICTED: 60S ribosomal protein L19-like	gi|532037025	63	4.7	1
76	Ribosomal protein S3, isoform CRA_f	gi|148684444	57	5.4	1
77	PREDICTED: dynein heavy chain 9, axonemal	gi|403275402	62	0.1	1
	Lysosome/melanosome/endosome				
1	Myosin-11	MYH11	166	2.9	4
2	Cathepsin K	CATK	105	11.5	3
3	Cathepsin D	CATD	91	6.8	2
4	Prosaposin	SAP	81	4.6	2
5	PREDICTED: cathepsin B isoform X1	gi|149698064	96	9.4	2
	Mitochondrion				
1	60 kDa heat shock protein, mitochondrial	CH60	167	14.0	5
2	Malate dehydrogenase, mitochondrial	MDHM	145	14.8	4
3	10 kDa heat shock protein, mitochondrial	CH10	87	29.4	3
4	Arginase-2, mitochondrial	ARGI2	67	3.4	1
5	Stress-70 protein, mitochondrial (Fragments)	GRP75	53	2.4	1
6	Aspartate aminotransferase, mitochondrial	AATM	67	2.8	1
	Golgi/ER lumen				
1	Protein disulfide-isomerase A3	PDIA3	573	27.5	14
2	Calumenin	CALU	374	40.0	9
3	Serpin H1	SERPH	367	27.3	9
4	Endoplasmin	ENPL	344	11.1	7
5	Calreticulin	CALR	257	24.7	8
6	Reticulocalbin-3	RCN3	154	12.5	3
7	Glucosidase 2 subunit beta	GLU2B	114	7.9	3
8	Endoplasmic reticulum resident protein 29	ERP29	92	11.1	3
9	Prolyl 4-hydroxylase subunit alpha-1	P4HA1	78	2.6	1
10	Proteasome-associated protein ECM29 homologue	ECM29	58	0.3	1
11	Thioredoxin domain-containing protein 5	TXND5	56	2.3	1
12	PREDICTED: reticulocalbin-1-like	gi|334331754	72	8.2	2
13	PREDICTED: hypoxia up-regulated protein 1	gi|514466500	62	2.1	1

Table 5. Continued

#	Name	Accession No.*	Mascot score	Seq. coverage (%)	No. of matched peptides
	Nucleus				
1	Neuroblast differentiation-associated protein AHNAK	AHNK	404	1.3	7
2	Nucleolin	NUCL	248	6.7	4
3	Prothymosin alpha	PTMA	198	22.7	4
4	Heterogeneous nuclear ribonucleoproteins A2/B1	ROA2	163	12.6	4
5	Heterogeneous nuclear ribonucleoprotein A/B	ROAA	163	13.0	3
6	Heterogeneous nuclear ribonucleoprotein D0	HNRPD	157	12.4	4
7	Heterogeneous nuclear ribonucleoprotein A1	ROA1	139	12.8	3
8	Thioredoxin	THIO	135	21.0	2
9	Plasminogen activator inhibitor 1 RNA-binding protein	PAIRB	132	6.6	2
10	High mobility group protein B1	HMGB1	129	17.7	3
11	Parathymosin	PTMS	120	22.5	3
12	Acidic leucine-rich nuclear phosphoprotein 32 family member A	AN32A	115	11.6	2
13	Peptidyl-prolyl cis-trans isomerase FKBP3	FKBP3	82	9.8	2
14	Synaptonemal complex protein 1	SYCP1	82	1.0	1
15	RNA-binding protein 3	RBM3	76	17.8	2
16	Lupus La protein homologue	LA	69	2.7	1
17	Nucleophosmin	NPM	65	4.8	1
18	Thyroid hormone receptor-associated protein 3	TR150	57	1.8	1
19	DDB1- and CUL4-associated factor 13	DCA13	57	1.8	1
20	DNA-binding protein	gi|181914	157	13.4	4
21	Ran/TC4 Binding Protein	gi|431422	65	5.4	1
22	PREDICTED: DDB1- and CUL4-associated factor 13	gi|348588727	59	1.8	1
	Contaminants				
1	Keratin, type II cytoskeletal 1	K2C1	380	13.8	8
2	Serum albumin	ALBU	168	5.8	3
3	Trypsin	TRYP	51	3.5	1
	Miscellaneous				
1	Coiled-coil domain-containing protein 18	CCD18	55	1.8	2
2	Outer dense fiberfibre protein 2-like	ODF2L	76	1.6	1
3	Chain C, Ternary Complex Of A Calcineurin A Fragment, Calcineurin B, Fkbp12 And The Immunosuppressant Drug Fk506 (tacrolimus)	gi|1942335	59	12.1	1
4	PREDICTED: 28 kDa heat- and acid-stable phosphoprotein	gi|149755423	59	11.0	1
5	PREDICTED: LOW QUALITY PROTEIN: 60S ribosomal protein L29-like	gi|513000456	60	5.2	1

*UniProt IDs are shown where available. In other cases, NCBInr accession numbers are shown.

Declaration of interest

References

Aigner T, Cook JL, Gerwin N, et al. (2010). Histopathology atlas of animal model systems – overview of guiding principles. Osteoarthritis Cartilage 18 Suppl 3:S2–6.

Almen MS, Nordstrom KJ, Fredriksson R, Schioth HB. (2009). Mapping the human membrane proteome: a majority of the human membrane proteins can be classified according to function and evolutionary origin. BMC Biol 7:50.

Archer CW, Francis-West P. (2003). The chondrocyte. Int J Biochem Cell Biol 35:401–4.

Barrett-Jolley R, Lewis R, Fallman R, Mobasheri A. (2010). The emerging chondrocyte channelome. Front Physiol 1:135.

Benz R. (1994). Permeation of hydrophilic solutes through mitochondrial outer membranes: review on mitochondrial porins. Biochim Biophys Acta 1197:167–96.

Bordier C. (1981). Phase separation of integral membrane proteins in Triton X-114 solution. J Biol Chem 256:1604–7.

Capra E, Beretta R, Parazzi V, et al. (2012). Changes in the proteomic profile of adipose tissue-derived mesenchymal stem cells during passages. Proteome Sci 10:46.

Cecil DL, Terkeltaub R. (2008). Transamidation by transglutaminase 2 transforms S100A11 calgranulin into a procatabolic cytokine for chondrocytes. J Immunol 180:8378–85.

Cordwell SJ, Thingholm TE. (2010). Technologies for plasma membrane proteomics. Proteomics 10:611–27.

De Pinto V, Messina A, Lane DJ, Lawen A. (2010). Voltage-dependent anion-selective channel (VDAC) in the plasma membrane. FEBS Lett 584:1793–9.

Diaz-Romero J, Gaillard JP, Grogan SP, et al. (2005). Immunophenotypic analysis of human articular chondrocytes: changes in surface markers associated with cell expansion in monolayer culture. J Cell Physiol 202:731–42.

Dissoki S, Abourbeh G, Salnikov O, et al. (2015). PET molecular imaging of angiogenesis with a multiple tyrosine kinase receptor-targeted agent in a rat model of myocardial infarction. Mol Imaging Biol 17:222–30.

Donato R, Cannon BR, Sorci G, et al. (2013). Functions of S100 proteins. Curr Mol Med 13:24–57.

Dunham J, Shackleton DR, Billingham MEJ, et al. (1988). A reappraisal of the structure of normal canine articular-cartilage. J Anat 157:89–99.

English JA, Manadas B, Scaife C, et al. (2012). Partitioning the proteome: phase separation for targeted analysis of membrane proteins in human post-mortem brain. PLoS One 7:e39509.

Garcia BA, Platt MD, Born TL, et al. (2006). Protein profile of osteoarthritic human articular cartilage using tandem mass spectrometry. Rapid Commun Mass Spectrom 20:2999–3006.

Hansson SF, Henriksson A, Johansson L, et al. (2010). Membrane protein profiling of human islets of langerhans using several extraction methods. Clin Proteom 6:195–207.

Hatakeyama Y, Hatakeyama J, Oka K, et al. (2014). Immunohistochemical study of amelogenin and lysosome-associate membrane proteins (LAMPs) in cartilage. Int J Morphol 32:618–26.

Hsueh MF, Onnerfjord P, Kraus VB. (2014). Biomarkers and proteomic analysis of osteoarthritis. Matrix Biol 39:56–66.

Kabbani N. (2008). Proteomics of membrane receptors and signaling. Proteomics 8:4146–55.

La Rocca G, Lo Iacono M, Corsello T, et al. (2013). Human Wharton's jelly mesenchymal stem cells maintain the expression of key immunomodulatory molecules when subjected to osteogenic, adipogenic and chondrogenic differentiation in vitro: new perspectives for cellular therapy. Curr Stem Cell Res Ther 8:100–13.

Lambrecht S, Dhaenens M, Almqvist F, et al. (2010). Proteome characterization of human articular chondrocytes leads to novel insights in the function of small heat-shock proteins in chondrocyte homeostasis. Osteoarthr Cartil 18:440–6.

Lambrecht S, Verbruggen G, Verdonk PC, et al. (2008). Differential proteome analysis of normal and osteoarthritic chondrocytes reveals distortion of vimentin network in osteoarthritis. Osteoarthr Cartil 16:163–73.

Lewis R, May H, Mobasheri A, Barrett-Jolley R. (2013). Chondrocyte channel transcriptomics: do microarray data fit with expression and functional data? Channels (Austin) 7:459–67

Mathias RA, Chen YS, Kapp EA, et al. (2011). Triton X-114 phase separation in the isolation and purification of mouse liver microsomal membrane proteins. Methods 54:396–406.

Matta C, Zakany R, Mobasheri A. (2015). Voltage-dependent calcium channels in chondrocytes: roles in health and disease. Curr Rheumatol Rep 17:43.

Mobasheri A. (2013). The future of osteoarthritis therapeutics: targeted pharmacological therapy. Curr Rheumatol Rep 15:364.

Mobasheri A, Carter SD, Martin-Vasallo P, Shakibaei M. (2002a). Integrins and stretch activated ion channels; putative components of functional cell surface mechanoreceptors in articular chondrocytes. Cell Biol Int 26:1–18.

Mobasheri A, Neama G, Bell S, et al. (2002b). Human articular chondrocytes express three facilitative glucose transporter isoforms: GLUT1, GLUT3 and GLUT9. Cell Biol Int 26:297–300.

Ode A, Schoon J, Kurtz A, et al. (2013). CD73/5'-ecto-nucleotidase acts as a regulatory factor in osteo-/chondrogenic differentiation of mechanically stimulated mesenchymal stromal cells. Eur Cell Mater 25:37–47.

Orazizadeh M, Salter DM. (2008). CD147 (extracellular matrix metalloproteinase inducer-emmprin) expression by human articular chondrocytes. Iran Biomed J 12:153–8.

Patti AM, Gabriele A, Della Rocca C. (1999). Human chondrocyte cell lines from articular cartilage of metatarsal phalangeal joints. Tissue Cell 31:550–4.

Rabilloud T. (2003). Membrane proteins ride shotgun. Nat Biotechnol 21:508–10.

Ruiz-Romero C, Carreira V, Rego I, et al. (2008). Proteomic analysis of human osteoarthritic chondrocytes reveals protein changes in stress and glycolysis. Proteomics 8:495–507.

Ruiz-Romero C, Lopez-Armada MJ, Blanco FJ. (2005). Proteomic characterization of human normal articular chondrocytes: a novel tool for the study of osteoarthritis and other rheumatic diseases. Proteomics 5:3048–59.

Samkoe KS, Tichauer KM, Gunn JR, et al. (2014). Quantitative in vivo immunohistochemistry of epidermal growth factor receptor using a receptor concentration imaging approach. Cancer Res 74:7465–74.

Sega EI, Low PS. (2008). Tumor detection using folate receptor-targeted imaging agents. Cancer Metastasis Rev 27:655–64.

Shakibaei M, Csaki C, Mobasheri A. (2008). Diverse roles of integrin receptors in articular cartilage. Adv Anat Embryol Cell Biol 197:1–60.

Suardita K, Fujimoto K, Oda R, et al. (2002). Effects of overexpression of membrane-bound transferrin-like protein (MTf) on chondrogenic differentiation in vitro. J Biol Chem 277:48579–86.

Sugimoto T, Yoshino M, Nagao M, et al. (1996). Voltage-gated ionic channels in cultured rabbit articular chondrocytes. Comp Biochem Physiol C Pharmacol Toxicol Endocrinol 115:223–32.

Tsolis KC, Bei ES, Papathanasiou I, et al. (2015). Comparative proteomic analysis of hypertrophic chondrocytes in osteoarthritis. Clin Proteomics 12:12.

Tsuga K, Tohse N, Yoshino M, et al. (2002). Chloride conductance determining membrane potential of rabbit articular chondrocytes. J Membr Biol 185:75–81.

Williams A, Smith JR, Allaway D, et al. (2011). Applications of proteomics in cartilage biology and osteoarthritis research. Front Biosci (Landmark Ed) 16:2622–44.

Williams A, Smith JR, Allaway D, et al. (2013). Carprofen inhibits the release of matrix metalloproteinases 1, 3, and 13 in the secretome of an explant model of articular cartilage stimulated with interleukin 1β. Arthritis Res Ther 15:R223.

Woods Jr VL, Schreck PJ, Gesink DS, et al. (1994). Integrin expression by human articular chondrocytes. Arthritis Rheum 37:537–44.

Wu J, Liu W, Bemis A, et al. (2007). Comparative proteomic characterization of articular cartilage tissue from normal donors and patients with osteoarthritis. Arthritis Rheum 56:3675–84.

Yan JX, Wait R, Berkelman T, et al. (2000). A modified silver staining protocol for visualization of proteins compatible with matrix-assisted laser desorption/ionization and electrospray ionization-mass spectrometry. Electrophoresis 21:3666–72.

Zhang ZJ, Peck SC. (2011). Simplified enrichment of plasma membrane proteins for proteomic analyses in *Arabidopsis thali*ana. Proteomics 11:1780–8.